# Quantum Phase Transitions in the Hubbard Model on a Triangular Lattice

Takuya Yoshioka,[1] Akihisa Koga,[2,3,4] and Norio Kawakami[2]

[1]*Department of Applied Physics, Osaka University, Suita, Osaka, 565-0871, Japan*
[2]*Department of Physics, Kyoto University, Kyoto 606-8502, Japan*
[3]*Theoretische Physik, ETH-Hönggerberg, Zürich 8093, Switzerland*
[4]*Department of Physics, Tokyo Institute of Technology, Tokyo 152-8551, Japan*

(Received 4 November 2008; published 16 July 2009)

We investigate the quantum phase transitions in the half-filled Hubbard model on the triangular lattice by means of the path-integral renormalization group method with a new iteration and truncation scheme proposed recently. It is found for a cluster of 36 sites that as the Hubbard interaction $U$ increases, the paramagnetic metallic state undergoes a first-order phase transition to a nonmagnetic insulating (NMI) state at $U_{c1} \sim 7.4t$, which is followed by another first-order transition to a 120° Néel ordered state at $U_{c2} \sim 9.2t$, where $t$ is the transfer integral. The size dependence of the results is also addressed. Our results suggest the existence of the intermediate NMI phase and resolve some controversial arguments on the nature of the previously proposed quantum phase transitions.

DOI: 10.1103/PhysRevLett.103.036401 PACS numbers: 71.10.Fd, 71.20.Rv, 71.30.+h

Strongly correlated electron systems with frustration have attracted much interest recently. There are a number of intriguing phenomena that have revealed new aspects of electron correlations. One of the striking examples can be found in an organic compound $\kappa$-(BEDT-TTF)$_2$Cu$_2$(CN)$_3$ [1–4], for which the triangular lattice structure of dimerized BEDT-TTF molecules plays an invaluable role in stabilizing a nonmagnetic spin-liquid insulating state down to 20 mK [4]. The nonmagnetic insulating (NMI) state, which is totally different from the naively expected 120° Néel ordered state [5,6], poses an interesting and challenging problem in the Mott transition of strongly correlated electrons on the frustrated triangular lattice [7–21]. In particular, it has been a central issue to figure out whether such a NMI state is really stabilized on the triangular lattice, and if so, how we can theoretically describe the Mott transition without any kind of magnetic ordering. The answer to the question should provide us with a deeper understanding of the Mott transition with strong frustration.

Low-energy properties of such frustrated organic compounds may be described by the single-band Hubbard model on the triangular lattice at half filling [1,7]. There have been a number of theoretical investigations on quantum phase transitions of the model [7–21]. However, most of conventional mean-field and variational treatments fail to describe the NMI phase, suggesting that the system may prefer the 120° Néel ordered state [18–20]. Among those intensive studies, the pioneering work by means of the path-integral renormalization group (PIRG) method [9] is believed to provide the most reliable results since it can fully incorporate quantum fluctuations on the basis of an unbiased scheme. By this method, Morita *et al.* reached the remarkable conclusion that the Mott transition occurs from the metallic state to the NMI state [9], and the corresponding transition may be continuous. Although the conclusion shed new light on the Mott transition, there still remain some questions/points: (i) Is such a continuous transition really possible in the fully frustrated system? (ii) The obtained critical value of the Hubbard interaction seems much smaller than the values deduced by other methods (see below). (iii) It is difficult to study the magnetic instability to the 120° Néel ordered phase by the naive PIRG method, so that it is unclear whether the NMI phase is indeed realized against the magnetic instability. We note that a more recent variational-cluster study found the metallic, NMI, and 120° Néel ordered phases in a certain parameter regime, but the transition points could not be estimated due to the problem of its numerical accuracy [19]. Therefore, it is highly desirable to precisely determine the ground-state phase diagram and clarify the nature of the associated quantum phase transitions in order to elucidate the essential properties inherent in the Mott transition under strong frustration.

In this Letter, we investigate the quantum phase transitions in the half-filled Hubbard model on the triangular lattice. By means of the PIRG method [22,23] with an improved iteration and truncation scheme proposed recently [24], we discuss how the NMI state competes with the metallic and 120° Néel ordered states. By computing the double occupancy, the momentum distribution function and the spin or charge correlation functions, we find that there are two successive quantum phase transitions among the metal–NMI–120° Néel ordered phases. The present results clearly predict the existence of the intermediate NMI phase and also shed light on some controversial arguments on the nature of the quantum phase transitions.

Let us consider the single-band Hubbard model on the triangular lattice. For simplicity, we adopt the square lattice with some diagonal bonds as shown in Fig. 1(b), which is topologically equivalent to the triangular lattice. The Hamiltonian we consider reads

 

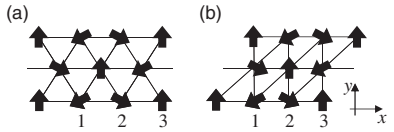


FIG. 1. (a) Triangular lattice and (b) square lattice with diagonal transfers, which is topologically equivalent to the original lattice (a). The arrows represent the spin configuration for the 120° Néel ordered state and the associated indices specify three different sublattices.

$$\hat{\mathcal{H}} = -t \sum_{\langle i,j\rangle,\sigma} (\hat{c}^{\dagger}_{i\sigma}\hat{c}_{j\sigma} + \text{H.c.}) + U\sum_{i} \hat{n}_{i\uparrow}\hat{n}_{i\downarrow}, \qquad (1)$$

where $\hat{c}_{i\sigma}$ ($\hat{c}^{\dagger}_{i\sigma}$) is an annihilation (creation) operator of an electron at the $i$th site with spin $\sigma$ ($=\uparrow, \downarrow$) and $\hat{n}_{i\sigma} = \hat{c}^{\dagger}_{i\sigma}\hat{c}_{i\sigma}$. $U$ ($>0$) is the Hubbard repulsion and $t$ ($>0$) is the nearest-neighbor transfer integral.

To study the ground-state properties of the Hubbard model Eq. (1), we use the PIRG method developed by Imada group [22,23]. The method is based on a simple idea that the true ground state $|\psi_g\rangle$ is obtained by acting the imaginary-time evolution operator on an initial state $|\phi_0\rangle$: $|\psi_g\rangle = e^{-\beta\hat{\mathcal{H}}}|\phi_0\rangle$ with $\beta \to \infty$. To approach the true ground state in the PIRG method, we operate $e^{-\Delta\tau\hat{\mathcal{H}}}$ with small $\Delta\tau$ on an approximate ground-state iteratively. This method is, in principle, independent of an initial state and an iterative scheme employed. However, how to choose them are crucial to reach the correct ground-state within restricted numerical resources. Here we use a new iteration and truncation scheme proposed in our previous paper [24], which is extremely efficient in performing the PIRG calculations with a large number of basis states. We examine various initial states deduced from unrestricted Hartree-Fock (UHF) solutions [25]. Besides, we further consider another class of initial states derived from UHF solutions in the spin-rotated frame where the quantization axis of spin is rotated with angles $\theta_0$, $\theta_0 + 2\pi/3$, and $\theta_0 + 4\pi/3$ respectively for three different sublattices (see Fig. 1). Performing the PIRG calculation with the initial states mentioned above, we discuss the ground-state properties of the Hubbard model on the triangular lattice. In this Letter, we carry out PIRG calculations for the half-filled systems with periodic boundary conditions ($N = 16$, 24, 30, and 36), where $N$ is the number of sites. In our PIRG calculations, we keep a large number of states (up to 500) as the Slater basis states, and fix $\Delta\tau/U = 0.5$. Our PIRG results for a small cluster ($N = 16$) are in good agreement with those obtained by the exact diagonalization (ED), as shown in Fig. 2. One of the remarkable advantages in our calculation is that our modified PIRG method with a new iteration scheme can cope with several competing states near the transition point properly as described in [24]. How to improve the initial states and extrapolate the true ground state is the same as in [24], though not shown in the figure.

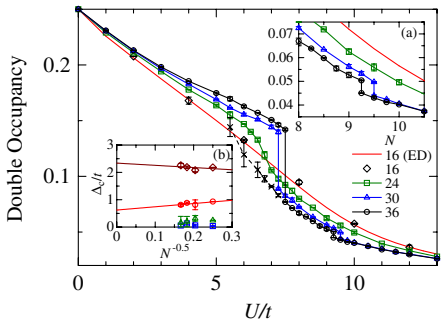


FIG. 2 (color online). The double occupancy as a function of $U/t$ for the half-filled Hubbard model on the triangular lattice. Crosses represent the results for the metastable state in the system ($N = 36$). The solid line represents the results obtained by the ED method. The inset (a) magnifies the double occupancy near $U_{c2}$ and (b) shows the finite size scaling of the charge excitation gap for $U/t = 3$ (squares), $U/t = 6$ (triangles), $U/t = 9$ (circles), and $U/t = 12$ (diamonds).

We first compute the expectation value of the double occupancy $\sum_{i=1}^{N}\langle\hat{n}_{i\uparrow}\hat{n}_{i\downarrow}\rangle/N$ [9]. Here, we focus on the results for the largest system ($N = 36$), which are shown as open circles in Fig. 2. The introduction of the repulsive interaction monotonically decreases the double occupancy, implying that the highly correlated metallic state is realized for $U < U_{c1}$. Further increase in the interaction gives rise to two successive discontinuities in the curve at $U = U_{c1}$ and $U_{c2}$ although the latter singularity is rather weak. We thus find that the double first-order quantum phase transitions occur in the system. This is also supported by the appearance of the two cusp singularities in the curve of the ground-state energy $E_g$, as shown in Fig. 3. By estimating the level crossing points of energies for the competing states, we determine the transition points $U_{c1}/t = 7.4 \pm 0.1$ and $U_{c2}/t = 9.2 \pm 0.3$.

To discuss how the ground-state properties depend on the system size, we also show the results for different clusters $N = 16$, 24, and 30 in Fig. 1. Two first-order

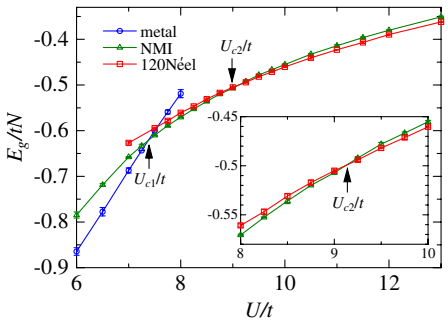


FIG. 3 (color online). The energies per site for the competing states in the half-filled Hubbard model on the triangular lattice ($N = 36$), where circles, triangles, and squares represent the energies for the metallic, NMI, and 120° Néel ordered states, respectively.

transitions do not occur in small clusters ($N = 16$ and 24), but appear clearly in the larger clusters ($N = 30$ and 36). Remarkably, the overall pattern of behavior is quite similar for $N = 30$ and 36, and the resulting transition points are little affected by the system size. We thus believe that the $N = 36$ system captures the essential properties of the model, and two successive transitions indeed occur even in the thermodynamic limit.

Having uncovered that double quantum phase transitions occur, let us now discuss the nature of the three distinct phases in detail. To clarify the nature of the transitions, we first calculate the charge excitation gap $\Delta_c$, which is defined as a difference between two chemical potentials, $\Delta_c = \frac{1}{2}(\mu_+ - \mu_-)$, where $\mu_\pm = \pm[E_g(N \pm 2) - E_g(N)]/2$. As shown in the inset (b) of Fig. 2, the finite charge excitation gap is clearly observed for $U > U_{c1}$, although its size in the thermodynamic limit is not easy to estimate precisely within the present numerical accuracy. This implies that the metal-insulator transition occurs at $U = U_{c1}$. We also calculate the momentum distribution function $n(\boldsymbol{q})$ and the momentum-dependent correlation function in the charge [spin] sector $N(\boldsymbol{q})$ [$S(\boldsymbol{q})$] [9]. These quantities are, respectively, given by the Fourier transform of the site-dependent correlation functions, $\langle \hat{c}^\dagger_{i\sigma}\hat{c}_{j\sigma}\rangle$, $(\langle \hat{n}_i\hat{n}_j\rangle - \langle \hat{n}_i\rangle\langle \hat{n}_j\rangle)$, and $\langle \hat{\boldsymbol{S}}_i \cdot \hat{\boldsymbol{S}}_j\rangle$, where $\hat{n}_i = \sum_\sigma \hat{n}_{i\sigma}$, $\hat{\boldsymbol{S}}_i = \frac{1}{2}\sum_{\alpha\beta}\hat{c}^\dagger_{i\alpha}\boldsymbol{\sigma}_{\alpha\beta}\hat{c}_{i\beta}$ and $\boldsymbol{\sigma}$ is the Pauli matrix. The computed results for the system ($N = 36$) are shown in Fig. 4. For $U < U_{c1}$, we find that the discontinuity exists in the momentum distribution function at the Fermi surface [Fig. 4(a)]. In this case, no singularity appears in the charge and spin correlation functions in Figs. 4(d) and 4(g). We thus confirm that the ordinary paramagnetic metallic state is stabilized for $U < U_{c1}$. On the other hand, when $U > U_{c1}$, the jump singularity disappears in the momentum distribution function, as shown in Figs. 4(b) and 4(c), in accordance with the Mott transition at $U = U_{c1}$. Correspondingly, the charge correlation function $N(\boldsymbol{q})$ changes its $|\boldsymbol{q}|$-dependence (small $|\boldsymbol{q}|$ region) from linear to quadratic. In the region $U_{c1} < U < U_{c2}$, the repulsive interaction enhances spin fluctuations at $\boldsymbol{q}_{\rm peak} = \pm(2\pi/3, 2\pi/3)$ characteristic of the 120° Néel ordered phase, but does not give rise to divergent behavior.

To discuss how magnetic fluctuations induce the 120° Néel ordered phase, we plot $S(\boldsymbol{q}_{\rm peak})$ as a function of $U/t$ for different choices of the system size in Fig. 5. In larger systems ($N = 30$ and 36), we find two clear jumps at $U_{c1}$ and $U_{c2}$ that signal the first-order phase transitions. Furthermore, it is clarified that spin fluctuations are strongly enhanced for $U > U_{c2}$, which suggests the emergence of the 120° Néel ordered phase. To discuss the stability of the 120° Néel ordered state, we also estimate the magnetization modulus defined by $M_N = [2S(\boldsymbol{q}_{\rm peak})/(N+6)]^{1/2}$ [5], which may be regarded as the order parameter in a finite cluster. In the strong coupling region ($U = 10t$), the magnetization modulus is estimated as

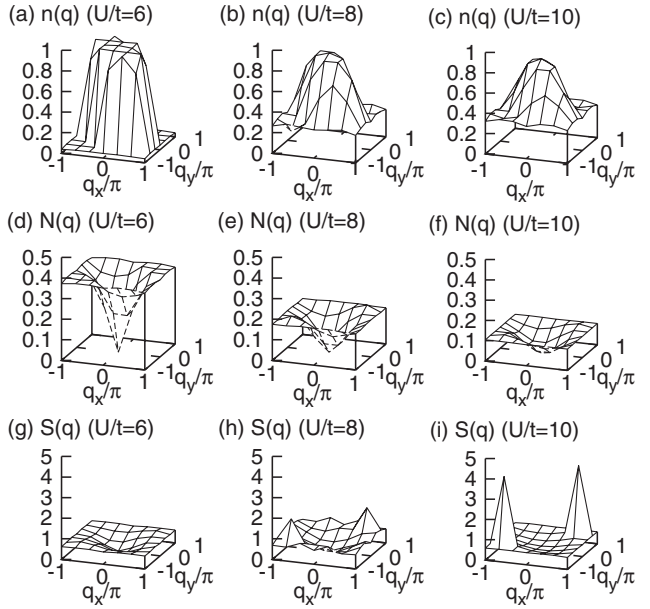


FIG. 4. The momentum distribution function $n(\boldsymbol{q})$, and the momentum-dependent charge [spin] correlation function $N(\boldsymbol{q})$ [$S(\boldsymbol{q})$] for the half-filled Hubbard model on the square lattice with $U/t = 6$, 8 and 10. For these values of interaction, the system is, respectively, in the metallic, NMI, and 120° Néel ordered phases. Note that the charge correlation shows the metallic behavior $N(\boldsymbol{q}) \sim |\boldsymbol{q}|$ in (d) and the insulating behavior $N(\boldsymbol{q}) \sim |\boldsymbol{q}|^2$ in (e) and (f).

$M_{36} = 0.43$, which is comparable to $M_{36} = 0.401$ for the Heisenberg model ($U/t \to \infty$) [5]. These observations naturally lead us to conclude that 120° Néel ordered phase is indeed realized for $U > U_{c2}$. In the intermediate phase $U_{c1} < U < U_{c2}$, we find in the inset of Fig. 5 that when the system size is increased, $S(\boldsymbol{q}_{\rm peak})$ is also enhanced. Because of the limited numerical resources, we could not reveal whether the spin structure factor diverges or saturates in the

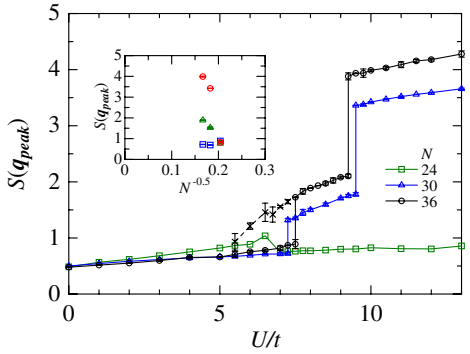


FIG. 5 (color online). The spin correlation function $S(\boldsymbol{q}_{\rm peak})$ as a function of $U/t$ for half-filled Hubbard model on the triangular lattice at half filling. Crosses represent the results for the metastable state in the system ($N = 36$). The inset shows the size dependence of $S(\boldsymbol{q}_{\rm peak})$ for $U/t = 6$ (squares), $U/t = 8$ (triangles), and $U/t = 10$ (circles).

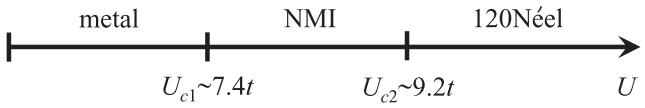


FIG. 6. Phase diagram for the half-filled Hubbard model on the triangular lattice ($N = 36$). Mott metal-insulator transition is of first order and magnetic transition is of weakly first order.

thermodynamic limit. However, its value is considerably smaller than that for the 120° Néel ordered phase ($U_{c2} < U$) and the jump singularity at $U = U_{c2}$ clearly appears in the larger clusters ($N = 30$, 36), as shown in Fig. 5. Therefore, we believe that in the intermediate phase, the spin structure factor should not diverge, the long-range order for the 120° spin correlations should be destroyed in the thermodynamic limit, and the NMI state is indeed realized between the metallic and 120° Néel ordered states.

It should be noted that the present results are in contrast to the previous PIRG results of Morita *et al.* [9]. First, our numerical data clearly demonstrate the first-order transition between the metal and insulator, while Morita *et al.* claimed that the transition may be continuous in the thermodynamic limit. Furthermore, the transition point $U_{c1} \sim 7.4t$ largely exceeds $U_c \sim 5.2t$ obtained in the latter work [9]. Second, our new PIRG algorithm can describe the 120° Néel ordered insulating phase which could not be treated in the previous study. Here we argue what really causes the difference between these PIRG results. In general, it is difficult to describe competing states in the coexistence region of first-order transitions on an equal footing. In particular, the PIRG results in the coexistence region strongly depend on the number of basis states employed. For example, the metallic ground state as well as the metastable insulating state can be found in terms of 500 basis states, but the former is missing in terms of 300 basis states in our treatment. We show a typical example of metastable insulating states in Figs. 2 and 5. Suppose we regard such a metastable state as the ground-state, the cusp singularity without discontinuity might appear in the curve of the double occupancy, as shown in Fig. 2. This would cause a misleading conclusion that the continuous Mott transition occurs around a small critical value $U_c \sim 5t$. Such pathological behavior becomes more serious when the system size is increased by keeping the number of basis states unchanged. We think that the results in Refs. [9,26] may suffer from a similar problem in the process of taking the thermodynamic limit (with 300 basis states). This analysis in turn elucidates that the present PIRG results are reliable up to the $N = 36$ cluster, which gives a practical limitation of our scheme. Nevertheless, we stress again that although our calculation is limited to such smaller system sizes, the reliable results obtained from 16 to 36 sites suggest the existence of two successive phase transitions in the thermodynamic limit.

We show our PIRG phase diagram in Fig. 6, which supports the existence of the NMI phase [9] and sheds light on the controversial arguments on the nature of the quantum phase transitions: The metal-insulator transition is not continuous but of first order, and the NMI phase proposed in Ref. [9] is indeed realized against the magnetic instability to the 120° Néel ordered phase.

Before concluding the Letter, we briefly comment on the nonmagnetic insulating state found in the organic compound $\kappa$-(BEDT-TTF)$_2$Cu$_2$(CN)$_3$. According to the band structure calculation [1], the transfer integral and the Coulomb interaction in the compound are estimated as $t \sim 54.5$ meV, $t' \sim 57.5$ meV, and $U \sim 448$ meV ($U/t \sim 8.2$ and $t'/t \sim 1.06$), so that the system is well described by the isotropic triangular lattice model. By exploiting these values, we conclude that the above compound with $U/t \sim 8.2$ is indeed in the NMI phase.

Parts of computations were done at the Super-computer Center at the Institute for Solid State Physics, University of Tokyo. This work was partly supported by the Grant-in-Aid for Scientific Research [20102008, 20029013, 21540359 (N. K.) and 20740194 (A. K.)] and the Global COE Programs "The Next Generation of Physics, Spun from Universality and Emergence"and "Nanoscience and Quantum Physics" from the Ministry of Education, Culture, Sports, Science and Technology (MEXT) of Japan.

[1] T. Komatsu *et al.*, J. Phys. Soc. Jpn. **65**, 1340 (1996).
[2] Y. Shimizu *et al.*, Phys. Rev. Lett. **91**, 107001 (2003).
[3] Y. Kurosaki *et al.*, Phys. Rev. Lett. **95**, 177001 (2005).
[4] S. Ohira *et al.*, J. Low Temp. Phys. **142**, 153 (2006).
[5] B. Bernu *et al.*, Phys. Rev. Lett. **69**, 2590 (1992).
[6] L. Capriotti *et al.*, Phys. Rev. Lett. **82**, 3899 (1999).
[7] H. Kino *et al.*, J. Phys. Soc. Jpn. **65**, 2158 (1996).
[8] Y. Imai *et al.*, Phys. Rev. B **65**, 233103 (2002).
[9] H. Morita *et al.*, J. Phys. Soc. Jpn. **71**, 2109 (2002).
[10] O. Parcollet *et al.*, Phys. Rev. Lett. **92**, 226402 (2004).
[11] S. S. Lee *et al.*, Phys. Rev. Lett. **95**, 036403 (2005).
[12] B. Kyung *et al.*, Phys. Rev. Lett. **97**, 046402 (2006).
[13] K. Aryanpour *et al.*, Phys. Rev. B **74**, 085117 (2006).
[14] T. Koretsune *et al.*, J. Phys. Soc. Jpn. **76**, 074719 (2007).
[15] T. Senthil, Phys. Rev. B **78**, 045109 (2008).
[16] T. Ohashi *et al.*, Phys. Rev. Lett. **100**, 076402 (2008).
[17] A. Liebsh *et al.*, Phys. Rev. B **78**, 165123 (2008).
[18] T. Watanabe *et al.*, Phys. Rev. B **77**, 214505 (2008).
[19] P. Sahebsara *et al.*, Phys. Rev. Lett. **100**, 136402 (2008).
[20] K. Inaba *et al.*, arXiv:0809.2383.
[21] D. Galanakis *et al.*, arXiv:0810.0001.
[22] M. Imada *et al.*, J. Phys. Soc. Jpn. **69**, 2723 (2000).
[23] T. Kashima *et al.*, J. Phys. Soc. Jpn. **70**, 2287 (2001).
[24] T. Yoshioka *et al.*, J. Phys. Soc. Jpn. **77**, 104702 (2008).
[25] N. Furukawa *et al.*, J. Phys. Soc. Jpn. **60**, 3669 (1991).
[26] S. Watanabe *et al.*, arXiv:0811.3718.